Distributed Formation Control of Nonholonomic Vehicles Subject to Velocity Constraints

Xiao Yu and Lu Liu, *Senior Member, IEEE*

***Abstract*—This paper considers a leader–follower formation control problem of nonholonomic vehicles of unicycle-type subject to velocity constraints. The velocity constraints of each vehicle are described by saturated angular velocity and bounded linear velocity lying between two positive constants. The communication topology of the networked multi-vehicle system is modeled by a directed graph. The designed control law is distributed in the sense that the controller of each follower vehicle only uses its own information and the information of its neighboring vehicles. It is shown that with the proposed control law, the leader–follower formation can be achieved without using absolute position measurements while the velocity constraints are satisfied. Finally, the simulation results of an example verify effectiveness of the proposed control law.**

***Index Terms*—Distributed formation control, nonholonomic vehicle, velocity constraint.**

I. Introduction

RECENT years have seen increased development in distributed control of multi-agent systems, see [1]–[6] and references therein. In particular, many researchers have shown great interest in the formation control of vehicles [6], [7]. The objective of formation control of vehicles is to make a team of vehicles move toward and maintain a desired geometric pattern, while maintaining a featured motion. In practice, vehicles are subject to the bounded maximum linear velocity due to thrust limitations and the saturated angular velocity due to steering rate limits. Besides, many vehicles are further subject to the constraint of the positive-minimum linear velocity due to stall conditions. In this case, vehicles can neither move backward directly nor slow down the linear velocity lower than a certain positive value. In fact, many ground vehicles and most aerial planes are subject to such physical velocity constraint, e.g., the fixed-wing unmanned aerial vehicle (UAV) [8]. Thus, it is of great theoretical and practical significance to investigate and develop distributed control approaches to vehicle formations subject to all aforementioned velocity constraints.

The leader–follower formation control problem refers to forcing follower vehicles to follow the leader's motion, while maintaining a desired geometric structure with respect to the leader. The special case with only one follower can be referred to as trajectory tracking control problem, which has been extensively studied in the literature, see [9]–[11]. To address all aforementioned velocity constraints in this special case, in [8], a controller was designed for a small fixed-wing UAV via selection from a feasible set which was defined by a constrained control Lyapunov function method. The authors in [12] considered the additive uncertainty and proposed a robust controller in terms of input-to-state stability. Unfortunately, the techniques from these works cannot be directly extended to formation control of multiple vehicles.

Nevertheless, many works studied the distributed formation control problem for multiple vehicles. In [13], the graph theory was used to develop a framework of modeling a formation by assuming a tree structure. Following this research, in [14], a nonlinear gain was employed to estimate the effect of the leader on formation. In [15], formation stability was analyzed by an approach based on control Lyapunov function method. In [16], the authors proposed a wiggling controller without using absolute position measurements, such that the stabilization of vehicle formation was achieved. In [17], collision avoidance and limited sensing range of vehicles were considered. In [18], a robust second-order sliding mode controller was proposed for the case where each follower knows the leader. In [19], to improve the convergence performance of formation tracking errors, the authors proposed a receding-horizon controller. All these works did not take into account any velocity constraints. Recently, velocity saturation of vehicles was considered in [20] and [21], and acceleration saturation was considered in [22].

However, the aforementioned works cannot be directly applied to the vehicles with positive-minimum linear velocity constraint. Several works did consider this constraint in the formation control problem in different cases. In [23], the authors studied formation control of unicycles with constrained line-of-sight angles. In [24], the case where one follower was required to stay in an arc of the circle centered in the frame of the leader was studied. In [25], a decentralized controller was proposed for the case where the leader maintains a uniform linear motion. Later in [26], the authors addressed the navigation problem without considering geometric formation. More recently, the authors in [27] and [28] used the small-gain method to design distributed controllers for the leader–follower formation, while the positive-minimum linear velocity constraint can be satisfied. The proposed controllers in [27] and [28] were based on static and time-varying relative position sensing digraphs, respectively. They both additionally required all followers to

Manuscript received February 25, 2015; revised August 9, 2015 and October 7, 2015; accepted October 27, 2015. Date of publication November 25, 2015; date of current version January 8, 2016. This work was supported by the Research Grants Council of the Hong Kong Special Administrative Region of China under Project CityU/11209514.

The authors are with the Department of Mechanical and Biomedical Engineering, City University of Hong Kong, Kowloon, Hong Kong SAR, China. (e-mail: xiaoyu4-c@my.cityu.edu.hk; luliu45@cityu.edu.hk).

Color versions of one or more of the figures in this paper are available online at http://ieeexplore.ieee.org.

Digital Object Identifier 10.1109/TIE.2015.2504042

have access to the real-time information of the leader through communication, including its heading angle, angular velocity, linear velocity, and linear acceleration.

In this paper, a novel distributed control law is developed for leader–follower formation of multiple nonholonomic vehicles subject to velocity constraints. From a distributed point of view, all vehicles are identical and anonymous. Each follower cannot identify the leader in general, and only has access to the local information and the information of its neighbors in a network of which the topology is modeled by a directed graph [1]. A dynamic control law is proposed, in which a distributed observer is developed such that the information associated with the leader can be estimated by each follower, and a velocity controller is designed to satisfy the velocity constraints. Finally, a technical lemma based on the cascaded system theory [29] is developed to show the uniform asymptotical stability of the closed-loop system.

The main features of the proposed distributed formation control law include 1) bounded functions are appropriately used such that the velocity constraints of each vehicle as described in [8] can always be satisfied and 2) compared with [27] and [28], the constraint of angular velocity is additionally taken into account, and any real-time information of the leader vehicle is not required to be known to all followers.

This paper is organized as follows. Section II presents the problem formulation and a technical lemma. In Section III, a distributed formation control law is proposed and stability analysis of the closed-loop system is presented. Section IV shows simulation results of an illustrative example, which is followed by the conclusion in Section V.

Notations and definitions: For a vector $x \in \mathbb{R}^n$, the norm $\|\cdot\|$ is defined as $\|x\| = \|x\|_2 = (\sum_{j=1}^{n} |x_i|^2)^{\frac{1}{2}}$.

II. Preliminaries

A. Problem Formulation

Consider a group of $N+1$ nonholonomic vehicles of unicycle type. For $i = 0, 1, \ldots, N$, the kinematic model of vehicle i is described by

$$\begin{aligned} \dot{x}_i &= v_i \cos\theta_i, \\ \dot{y}_i &= v_i \sin\theta_i, \\ \dot{\theta}_i &= \omega_i, \end{aligned} \tag{1}$$

where $[x_i \; y_i]^\top \in \mathbb{R}^2$ is the Cartesian coordinates of the center of mass (absolute position) and $\theta_i \in \mathbb{R}$ is the heading angle (orientation) in the inertial frame. $v_i \in \mathbb{R}$ and $\omega_i \in \mathbb{R}$ are the linear velocity and angular velocity, respectively, which are regarded as the control inputs. It is noticed that, in practice, θ_i and $\theta_i + 2K_i\pi$ with $K_i \in \mathbb{Z}$ represent the same orientation.

The following physical velocity constraints are considered:

$$v_i \in [v_{\min},\, v_{\max}], \quad v_{\max} > v_{\min} > 0, \tag{2}$$

$$\omega_i \in [-\omega_{\max},\, \omega_{\max}], \quad \omega_{\max} > 0. \tag{3}$$

In the desired vehicle formation, all vehicles move with the group reference velocities $v_r(t)$ and $\omega_r(t)$. Note that $v_r(t) \in [v_r^-,\, v_r^+] \subset [v_{\min},\, v_{\max}]$ and $\omega_r(t) \in [-\omega_r^+,\, \omega_r^+] \subset [-\omega_{\max},\, \omega_{\max}]$, where v_r^-, v_r^+, ω_r^+ and $v_{\min}$, $v_{\max}$, $\omega_{\max}$ are known constants.

The leader–follower formation control problem is considered in this paper. The group of vehicles contains one uncontrolled vehicle labeled 0, and it is called leader. The others labeled i, $i = 1, \ldots, N$, are followers. All vehicles are identical, and followers cannot identify the leader. All follower vehicles are required to follow the leader's motion while maintaining a desired geometric structure. The leader which decides the group reference velocities satisfies the following assumption.

[A1] $v_0(t)$ and $\omega_0(t)$ are bounded, i.e., $v_0(t) \in [v_0^-,\, v_0^+]$, $\omega_0(t) \in [\omega_0^-,\, \omega_0^+]$, $\forall t \geq 0$, where $[v_0^-,\, v_0^+] \subseteq [v_r^-,\, v_r^+]$ and $[\omega_0^-,\, \omega_0^+] \subseteq [-\omega_r^+,\, \omega_r^+]$.

In practice, the linear acceleration of a vehicle is bounded and thus the following assumption is made as in [27] and [28]:

[A2] $\dot{v}_0(t)$ exists and is bounded for all $t \geq 0$.

As in [27], the leader is assumed to know its own linear velocity v_0, angular velocity ω_0, and linear acceleration $\dot{v}_0$. The objective of the leader–follower formation control problem is to design a controller for vehicle i, $i = 1, \ldots, N$, such that $[x_i(t) \; y_i(t)]^\top$ converges to $[x_0(t) + d_{i0}^x \; y_0(t) + d_{i0}^y]^\top$ and $\theta_i(t)$ converges to $\theta_0(t) + 2K_i\pi$ with $K_i \in \mathbb{Z}$, where the constant vector $\boldsymbol{d}_{i0} := [d_{i0}^x \; d_{i0}^y]^\top$ denotes the desired relative position to the leader. By default, $\boldsymbol{d}_{00} = 0$. Each follower vehicle i does not know d_{i0}, but knows the desired relative position to its neighboring vehicle j, i.e., $\boldsymbol{d}_{ij} := [d_{ij}^x \; d_{ij}^y]^\top$.

The network among vehicles is physically set up by the onboard sensor and communication device of each vehicle. Since the absolute positions of vehicles are usually unavailable [27], [28], the sensor of a vehicle can only measure the relative positions to its neighbors in the network. The communication devices of vehicles provide the information transmission among vehicles. Each vehicle only has access to the information of its neighbors in the network. The topology of this network is described by a directed graph $\bar{\mathcal{G}}$ as follows.

First, a directed graph $\mathcal{G} = \{\mathcal{O}, \mathcal{E}\}$ is used to describe the network among N followers. The digraph $\mathcal{G}$ consists of a finite set of nodes $\mathcal{O} = \{1, \ldots, N\}$ representing N followers, and a set of edges $\mathcal{E} = \{(j, i) : j \neq i, i, j \in \mathcal{O}\}$ containing directed edges from node j to node i. Next, combining $\mathcal{G}$ and node 0 (leader) yields the digraph $\bar{\mathcal{G}} = \{\bar{\mathcal{O}}, \bar{\mathcal{E}}\}$, where $\bar{\mathcal{O}} = \mathcal{O} \cup \{0\}$, and $\bar{\mathcal{E}}$ includes $\mathcal{E}$ and directed edges from node 0 to node i, $i \in \mathcal{O}$. A directed edge (j, i) $(j \neq i, j \in \bar{\mathcal{O}}, i \in \mathcal{O})$ means that vehicle i can have access to the information of vehicle j. Node j is a neighbor of node i if $(j, i) \in \bar{\mathcal{E}}$, and a set $\mathcal{N}_i \subseteq \bar{\mathcal{O}}$ denotes all neighbors of node i. Finally, define $a_{ij} = 1$ if $(j, i) \in \bar{\mathcal{E}}$, otherwise $a_{ij} = 0$. The following assumption is made on the digraph $\bar{\mathcal{G}}$.

[A3] The digraph $\bar{\mathcal{G}}$ contains a directed spanning tree with node 0 being the root.

Now, the leader–follower formation control problem considered in this paper is formally defined as follows.

Definition 2.1: Consider N follower vehicles and a leader vehicle, and define the formation tracking errors as

$$e_i^x = x_0 - x_i + d_{i0}^x,\; e_i^y = y_0 - y_i + d_{i0}^y,\; e_i^\theta = \theta_0 - \theta_i. \tag{4}$$

Given a digraph $\bar{\mathcal{G}}$, for all initial states $[e_i^x(t_0)\ e_i^y(t_0)]^\top \in \mathbb{R}^2$ and $e_i^\theta(t_0) \in (-2\pi, 2\pi)$, $\forall t_0 \geq 0$, find a dynamic control law in the form of

$$\dot{\rho}_i = \varrho(x_j - x_i, y_j - y_i, \theta_i, \rho_i, \rho_j, \boldsymbol{d}_{ij}), \tag{5}$$

$$[v_i\ \omega_i]^\top = \sigma(\rho_i, \theta_i),\ j \in \mathcal{N}_i, \quad i = 1, \ldots, N, \tag{6}$$

such that

$$\lim_{t\to\infty} e_i^x(t) = 0,\ \lim_{t\to\infty} e_i^y(t) = 0,\ \lim_{t\to\infty} e_i^\theta(t) = 0, \tag{7}$$

where ρ_i, to be designed later, is an estimate of the information associated with the leader, $\boldsymbol{d}_{ij} = [d_{ij}^x\ d_{ij}^y]^\top$ is the desired relative position between vehicles i and j, functions $\varrho(\cdot)$ and $\sigma(\cdot)$ are sufficiently smooth, and $\sigma(\cdot)$ is properly bounded subject to (2) and (3).

Remark 2.1: Since $e_i^\theta(t_0)$ represents the same orientation as $e_i^\theta(t_0) + 2K_i\pi \in \mathbb{R}$ with any $K_i \in \mathbb{Z}$, $(-2\pi, 2\pi)$ covers all orientations. In fact, the measurement θ_i from the sensors such as IMU/compass or gyroscope [30] usually returns a value in $[0, 2\pi)$ or $(-\pi, \pi]$, which results in $e_i^\theta \in (-2\pi, 2\pi)$.

Remark 2.2: The problem setup does not include collision avoidance, and vehicles may be assumed to move on different altitudes such that collision will not happen. Approaches to avoiding collisions will be investigated in future.

B. A Technical Lemma

Before presenting the main results, a technical lemma is given. This lemma is motivated by the cascaded system theory presented in [29] and will be used in the stability analysis of the closed-loop system.

Consider the following system:

$$\dot{\chi} = f(\chi, \gamma(t)) + g(\chi, \xi, \gamma(t)), \tag{8}$$

where $\chi \in \mathbb{R}^n$ is the state, $\xi \in \mathbb{R}^m$ is an exogenous signal, $\gamma : \mathbb{R}_{\geq 0} \mapsto \Gamma$ are time-varying functions, and Γ is a compact subset of $\mathbb{R}^q$. Functions $f(\chi, \gamma(t))$ and $g(\chi, \xi, \gamma(t))$ are continuous in their arguments. $f(\chi, \gamma(t))$ is locally Lipschitz on χ uniformly on γ [31], i.e., for each compact subset $\mathbb{K}$, $\mathbb{K} \in \mathbb{R}^n$, there is some constant c such that $\|f(X, \bar{\gamma}) - (Y, \bar{\gamma})\| \leq c\|X - Y\|$ for all $X,\ Y \in \mathbb{K}$ and all $\bar{\gamma} \in \Gamma$. $g(\chi, \xi, \gamma(t))$ is locally Lipschitz on (χ, ξ) uniformly on γ. System (8) can be considered as a perturbation of the nominal system

$$\dot{\chi} = f(\chi, \gamma(t)). \tag{9}$$

As shown later, the closed-loop system consisting of each follower (1) and the proposed control law can be written in the form of (8), and the perturbation term $g(\chi, \xi, \gamma(t))$ results from the inter-vehicle information exchange.

In particular, the following lemma gives sufficient conditions to guarantee that a uniformly asymptotically stable nonlinear system (9) remains uniformly asymptotically stable when it is perturbed by $g(\chi, \xi, \gamma(t))$ under some conditions.

Lemma 2.1: Let $\chi = 0$ be an equilibrium point for system (8). If the following conditions [C1]–[C3] are satisfied, system (8) is globally uniformly asymptotically stable at $\chi = 0$.

[C1] The nominal system (9) is globally uniformly asymptotically stable with a Lyapunov function $V : \mathbb{R}_{\geq 0} \times \mathbb{R}^n \mapsto \mathbb{R}_{\geq 0}$, such that for all $t \geq 0$ and all $\chi \in \mathbb{R}^n$,

$$\underline{W}(\chi) \leq V(t, \chi) \leq \overline{W}(\chi), \tag{10}$$

?

$$\frac{\partial V(t, \chi)}{\partial t} + \frac{\partial V(t, \chi)}{\partial \chi} f(\chi, \gamma(t)) \leq -W(\chi), \tag{11}$$

$$\left\|\frac{\partial V(t, \chi)}{\partial \chi}\right\| \|\chi\| \leq c_1 V(t, \chi), \quad \forall \|\chi\| \geq \zeta, \tag{12}$$

$$\left\|\frac{\partial V(t, \chi)}{\partial \chi}\right\| \leq c_2, \quad \forall \|\chi\| \leq \zeta, \tag{13}$$

strictly inc.

$f(0)=0$

$\lim_{r\to\infty} f(r) = \infty$

where $\underline{W}(\chi)$ and $\overline{W}(\chi)$ are two class $\mathcal{K}_\infty$ functions, $W(\chi)$ is a *positive semi-definite* function, and $c_1 > 0$, $\zeta > 0$, and $c_2 > 0$ are some constants.

$f(r,s) \to$ fix $s \to f \in \mathcal{K}$, fix $r \to f$ is decreasing wrt s. $\lim_{s\to\infty} f = 0$

[C2] There exists a class $\mathcal{KL}$ function $\varphi(\cdot)$ and a class $\mathcal{K}$ function $\phi(\cdot)$, such that for all $t \geq t_0 \geq 0$ and all $\xi(t_0) \in \mathbb{R}^m$,

$$\|\xi(t)\| \leq \varphi(\|\xi(t_0)\|, t - t_0),\ \int_{t_0}^{\infty} \|\xi(t)\| dt \leq \phi(\|\xi(t_0)\|). \tag{14}$$

[C3] The function $g(\chi, \xi, \gamma(t))$ satisfies that for all $\chi \in \mathbb{R}^n$ and all $\xi \in \mathbb{R}^m$, (Perturbation has to be small)

$$\|g(\chi, \xi, \gamma(t))\| \leq \|\xi\| \left(\Theta_1(\|\xi\|) + \|\chi\|\Theta_2(\|\xi\|)\right), \tag{15}$$

where $\Theta_1,\ \Theta_2 : \mathbb{R}_{\geq 0} \mapsto \mathbb{R}_{\geq 0}$ are continuous functions.

A sketch of the proof is given in the Appendix.

For the case where system (9) is uniformly asymptotically stable in a domain $\mathcal{X} \subset \mathbb{R}^n$ containing $\chi = 0$ and $\xi(t) \to 0$ exponentially as $t \to 0$, the following corollary holds.

Corollary 2.1: Let $\chi = 0$ be an equilibrium point for system (8) and $\mathcal{X} \subset \mathbb{R}^n$ be a domain containing $\chi = 0$. System (8) is uniformly asymptotically stable for $\chi \in \mathcal{X}$, if (i) the nominal system (9) is uniformly asymptotically stable for $\chi \in \mathcal{X}$ with a Lyapunov function $V : \mathbb{R}_{\geq 0} \times \mathcal{X} \mapsto \mathbb{R}_{\geq 0}$, and two class $\mathcal{K}$ functions $\underline{W}, \overline{W} : \mathcal{X} \mapsto \mathbb{R}_{\geq 0}$, such that (10)–(13) hold for any $\chi \in \mathcal{X}$; (ii) there exist positive constants k and ς such that for any initial state $\xi(t_0) \in \mathbb{R}^m$, $\|\xi(t)\| \leq k\|\xi(t_0)\|e^{-\varsigma(t-t_0)}$; (iii) [C3] holds for any $\chi \in \mathcal{X}$ and $\xi \in \mathbb{R}^m$.

III. Main Results

In this section, the main results will be presented in two steps. First, a distributed observer in the form of (5) is developed for each follower such that the information associated with the leader can be estimated, including e_i^x, e_i^y, θ_0, ω_0, and v_0. Second, a velocity controller is designed in the form of (6) such that leader–follower formation can be achieved, while the velocity constraints (2) and (3) are always satisfied.

For simplicity, convert the tracking errors (4) expressed in the inertial frame to those in the Frenet–Serret frame of vehicle i by using the following coordinate transformation [32]:

$$\begin{bmatrix} x_{ei} \\ y_{ei} \end{bmatrix} = R(\theta_i) \begin{bmatrix} e_i^x \\ e_i^y \end{bmatrix},\ R(\theta_i) = \begin{bmatrix} \cos\theta_i & \sin\theta_i \\ -\sin\theta_i & \cos\theta_i \end{bmatrix},$$

$$\theta_{ei} = e_i^\theta, \tag{16}$$

local body frame

which yields the following error dynamics:

$$\begin{aligned} \dot{x}_{ei} &= \omega_i y_{ei} - v_i + v_0 \cos\theta_{ei}, \\ \dot{y}_{ei} &= -\omega_i x_{ei} + v_0 \sin\theta_{ei}, \\ \dot{\theta}_{ei} &= \omega_0 - \omega_i. \end{aligned} \tag{17}$$

Thus, to show (7), it suffices to show that for all initial states $[x_{ei}(t_0)\ y_{ei}(t_0)]^{\mathrm{T}} \in \mathbb{R}^2$ and $\theta_{ei}(t_0) \in (-2\pi,\ 2\pi)$, $\forall t_0 \geq 0$,

$$\lim_{t\to\infty} x_{ei}(t) = 0,\ \lim_{t\to\infty} y_{ei}(t) = 0,\ \lim_{t\to\infty} \theta_{ei}(t) = 0.$$

A. Distributed Observer Design

Since each follower has no knowledge of the information associated with the leader directly, the error $[x_{ei}\ y_{ei}\ \theta_{ei}]^{\mathrm{T}}$ and the velocities of the leader $[v_0\ \omega_0]^{\mathrm{T}}$ cannot be directly used in the controller design. Thus, a dynamic observer is developed for each follower, such that $[x_{ei}\ y_{ei}\ \theta_{ei}]^{\mathrm{T}}$ and $[v_0\ \omega_0]^{\mathrm{T}}$ can be estimated. This observer is designed as follows.

First, assign a virtual leader vehicle with state $[\hat{x}_i\ \hat{y}_i\ \hat{\theta}_i]^{\mathrm{T}}$ and velocity $[\hat{v}_i\ \dot{\hat{\theta}}_i]^{\mathrm{T}}$ for each follower vehicle.

Trying to estimate state of leader $(\bar{x}_0)$

Then, define $\hat{e}_i := [\hat{e}_i^x\ \hat{e}_i^y]^{\mathrm{T}}$ and $\hat{e}_i^\theta$ as

$$\hat{e}_i^x = \hat{x}_i - x_i + d_{i0}^x,\ \hat{e}_i^y = \hat{y}_i - y_i + d_{i0}^y,\ \hat{e}_i^\theta = \hat{\theta}_i - \theta_i. \tag{18}$$

Note that the absolute position $[x_i\ y_i]^{\mathrm{T}}$ is not measurable and $[d_{i0}^x\ d_{i0}^y]^{\mathrm{T}}$ is not known to vehicle i. $\hat{e}_i$ is used to estimate the formation tracking error $[e_i^x\ e_i^y]^{\mathrm{T}}$ defined in (4), such that $[x_{ei}\ y_{ei}]^{\mathrm{T}}$ can be estimated.

If assumptions [A2] and [A3] hold, $\dot{v}_0$ exists and $\sum_{j\in\mathcal{N}_i} a_{ij} \neq 0$. Then, design a dynamic observer for each follower as

$$\begin{aligned} \dot{\hat{e}}_i^x &= \hat{v}_i \cos\hat{\theta}_i - v_i \cos\theta_i \\ &\quad + \sum_{j\in\mathcal{N}_i} a_{ij}\left((\hat{e}_j^x - \hat{e}_i^x) + (x_j - x_i) + d_{ij}^x\right), \end{aligned} \tag{19}$$

$$\begin{aligned} \dot{\hat{e}}_i^y &= \hat{v}_i \sin\hat{\theta}_i - v_i \sin\theta_i \\ &\quad + \sum_{j\in\mathcal{N}_i} a_{ij}\left((\hat{e}_j^y - \hat{e}_i^y) + (y_j - y_i) + d_{ij}^y\right), \end{aligned} \tag{20}$$

$$\ddot{\hat{\theta}}_i = \frac{1}{\sum\limits_{j\in\mathcal{N}_i} a_{ij}} \sum_{j\in\mathcal{N}_i} a_{ij}\ddot{\hat{\theta}}_j + \frac{1}{\sum\limits_{j\in\mathcal{N}_i} a_{ij}} \sum_{j\in\mathcal{N}_i} a_{ij}(\dot{\hat{\theta}}_j - \dot{\hat{\theta}}_i), \tag{21}$$

$$\dot{\hat{v}}_i = \frac{1}{\sum\limits_{j\in\mathcal{N}_i} a_{ij}} \sum_{j\in\mathcal{N}_i} a_{ij}\dot{\hat{v}}_j + \frac{1}{\sum\limits_{j\in\mathcal{N}_i} a_{ij}} \sum_{j\in\mathcal{N}_i} a_{ij}(\hat{v}_j - \hat{v}_i). \tag{22}$$

The information of the ith observer $[\hat{e}_i\ \hat{\theta}_i\ \hat{v}_i\ \dot{\hat{\theta}}_i\ \dot{\hat{v}}_i]^{\mathrm{T}}$ can be viewed as an internal state of vehicle i. By default, $[\hat{e}_0\ \hat{\theta}_0\ \hat{v}_0\ \dot{\hat{\theta}}_0\ \dot{\hat{v}}_0]^{\mathrm{T}} = [0\ \theta_0\ v_0\ \omega_0\ \dot{v}_0]^{\mathrm{T}}$. For each follower, the observer design uses the local information and information of its neighbors, and thus the observer design is distributed.

The inter-vehicle information exchange with observer (19)–(22) can be implemented as follows. If vehicle j is the neighbor of vehicle i, the sensor of vehicle i measures its relative position to vehicle j, i.e., $[x_j - x_i\ y_j - y_i]^{\mathrm{T}}$, instead of its own absolute position $[x_i\ y_i]^{\mathrm{T}}$. Meanwhile, the communication device of vehicle i can receive the information $[\hat{e}_j\ \hat{\theta}_j\ \hat{v}_j\ \dot{\hat{\theta}}_j\ \dot{\hat{v}}_j]^{\mathrm{T}}$ from vehicle j. All vehicles measure and receive their respective information based on the topology of digraph $\bar{\mathcal{G}}$. The distributed observer (19)–(22) owns a property stated in the following lemma.

Lemma 3.1: Consider the distributed observer (19)–(22), the leader vehicle, and the digraph $\bar{\mathcal{G}}$. Under assumptions [A1]–[A3], for any initial states $\hat{e}_i(t_0)$, $\hat{\theta}_i(t_0)$, $\hat{v}_i(t_0)$, $\dot{\hat{\theta}}_i(t_0)$, $\dot{\hat{v}}_i(t_0)$, $i = 0, 1, \ldots, N$, $\forall t_0 \geq 0$, $\hat{e}_i(t) \to [e_i^x(t)\ e_i^y(t)]^{\mathrm{T}}$, $\hat{\theta}_i(t) \to \theta_0(t)$, $\dot{\hat{\theta}}_i(t) \to \omega_0(t)$, and $\hat{v}_i(t) \to v_0(t)$ *exponentially* as $t \to \infty$.

Proof: Define

$$\tilde{x}_i = \hat{x}_i - x_0,\ \tilde{y}_i = \hat{y}_i - y_0,\ \tilde{\theta}_i = \hat{\theta}_i - \theta_0,\ \tilde{v}_i = \hat{v}_i - v_0, \tag{23}$$

$$\nu_i^x = \hat{v}_i \cos\hat{\theta}_i - v_0 \cos\theta_0,\ \nu_i^y = \hat{v}_i \sin\hat{\theta}_i - v_0 \sin\theta_0, \tag{24}$$

and denote $\tilde{x} = \mathrm{col}(\tilde{x}_1, \ldots, \tilde{x}_N)$, $\tilde{y} = \mathrm{col}(\tilde{y}_1, \ldots, \tilde{y}_N)$, $\tilde{\theta} = \mathrm{col}(\tilde{\theta}_1, \ldots, \tilde{\theta}_N)$, $\tilde{v} = \mathrm{col}(\tilde{v}_1, \ldots, \tilde{v}_N)$, $\nu^x = \mathrm{col}(\nu_1^x, \ldots, \nu_N^x)$, and $\nu^y = \mathrm{col}(\nu_1^y, \ldots, \nu_N^y)$.

First, it will show that $\hat{\theta}_i(t) \to \theta_0(t)$, $\dot{\hat{\theta}}_i(t) \to \omega_0(t)$, and $\hat{v}_i(t) \to v_0(t)$ exponentially as $t \to \infty$.

It follows from (21) that for $i = 1, \ldots, N$,

$$\sum_{j\in\mathcal{N}_i} a_{ij}(\ddot{\hat{\theta}}_i - \ddot{\hat{\theta}}_j) = -\sum_{j\in\mathcal{N}_i} a_{ij}(\dot{\hat{\theta}}_i - \dot{\hat{\theta}}_j). \tag{25}$$

Define $\Delta_i = \sum_{j\in\mathcal{N}_i} a_{ij}(\dot{\hat{\theta}}_i - \dot{\hat{\theta}}_j)$ and (25) can be rewritten as

$$\dot{\Delta}_i = -\Delta_i,\ i = 1, \ldots, N. \tag{26}$$

Then, one can obtain $\Delta_i(t) = e^{-(t-t_0)}\Delta_i(t_0)$.

Note that the Laplacian matrix $\bar{\mathcal{L}}$ of the digraph $\bar{\mathcal{G}}$ can be partitioned as follows:

$$\bar{\mathcal{L}} = \left(\begin{array}{c|c} \sum_{j=1}^N a_{0j} & [a_{01}, \ldots, a_{0N}] \\ \hline -\mathcal{A}_0\mathbf{1}_N & H \end{array}\right), \tag{27}$$

where $\mathcal{A}_0 = \mathrm{diag}\{a_{10}, \ldots, a_{N0}\}$. Noting that there exist no directed edges from followers to the leader in the digraph $\bar{\mathcal{G}}$, thus $\sum_{j=1}^N a_{0j} = 0$ and $[a_{01}, \ldots, a_{0N}] = 0$.

Denote $\dot{\hat{\theta}} = \mathrm{col}(\dot{\hat{\theta}}_1, \ldots, \dot{\hat{\theta}}_N)$. Since $\dot{\hat{\theta}}_0 = \dot{\theta}_0$, one can obtain

$$[\Delta_1, \ldots, \Delta_N]^{\mathrm{T}} = H(\dot{\hat{\theta}} - \mathbf{1}_N \otimes \dot{\theta}_0) = H\dot{\tilde{\theta}}. \tag{28}$$

By assumption [A3] and Lemma 1 in [4], H is nonsingular and all eigenvalues of H have positive real parts. Thus, $-H$ is Hurwitz. Since $\Delta_i(t) = e^{-(t-t_0)}\Delta_i(t_0)$, it follows from (28) that $\dot{\tilde{\theta}}(t) \to 0$. Thus, $\dot{\hat{\theta}}_i(t) \to \dot{\theta}_0(t)$ exponentially as $t \to \infty$.

Denote $\ddot{\hat{\theta}} = \mathrm{col}(\ddot{\hat{\theta}}_1, \ldots, \ddot{\hat{\theta}}_N)$. Since $\ddot{\hat{\theta}}_0 = \dot{\omega}_0$, one can obtain

$$\left[\dot{\Delta}_1, \ldots, \dot{\Delta}_N\right]^{\mathrm{T}} = H(\ddot{\hat{\theta}} - \mathbf{1}_N \otimes \dot{\omega}_0). \tag{29}$$

It follows from (26) that $\dot{\Delta}_i(t) \to 0$ exponentially as $t \to \infty$. Then, $\dot{\hat{\theta}}_i(t) \to \omega_0(t)$ exponentially as $t \to \infty$. Similarly, it can be shown that $\hat{v}_i(t) \to v_0(t)$ exponentially as $t \to \infty$.

Second, to show $\hat{e}_i(t) \to [e_i^x(t)\ e_i^y(t)]^\top$ exponentially as $t \to \infty$, it suffices to show that $\|\hat{x}_i(t) - x_0(t)\| \to 0$ and $\|\hat{y}_i(t) - y_0(t)\| \to 0$ exponentially as $t \to \infty$.

Using (18)–(20) and $[d_{ij}^x\ d_{ij}^y]^\top = [d_{i0}^x - d_{j0}^x\ d_{i0}^y - d_{j0}^y]^\top$, one can obtain

$$\dot{\tilde{x}} = \nu^x - H\tilde{x}, \quad \dot{\tilde{y}} = \nu^y - H\tilde{y}, \tag{30}$$

where H is defined in (27). Since $-H$ is Hurwitz, there exist $\alpha,\ \beta > 0$, such that

$$\|e^{-Hs}\| \le \alpha e^{-\beta s}, \quad \forall s \ge 0. \tag{31}$$

Since $\nu_i^x = (\hat{v}_i - v_0)\cos\hat{\theta}_i + v_0(\cos\hat{\theta}_i - \cos\theta_0)$ and $\cos(\cdot)$ is Lipschitz continuous, there exists an $l_c > 0$, such that $\|\nu^x(t)\| \le \|\tilde{v}(t)\| + l_c v_0^+ \|\tilde{\theta}(t)\|$. Since $\hat{\theta}_i(t) \to \theta_0(t)$ and $\hat{v}_i(t) \to v_0(t)$ exponentially as $t \to \infty$, then there exist $\alpha_1,\ \alpha_2,\ \beta_1,\ \beta_2 > 0$, such that for all $t \ge t_0 \ge 0$,

$$\|\tilde{v}(t)\| \le \alpha_1 e^{-\beta_1 t}\|\tilde{v}(t_0)\|,\ l_c v_0^+ \|\tilde{\theta}(t)\| \le \alpha_2 e^{-\beta_2 t}\|\tilde{\theta}(t_0)\|. \tag{32}$$

Then, it follows from (30) and (31) that

$$\begin{aligned}\|\tilde{x}(t)\| &= \|e^{-H(t-t_0)}\tilde{x}(t_0) + \int_{t_0}^t e^{-H(t-\tau)}\nu^x(\tau)d\tau\| \\ &\le \|e^{-H(t-t_0)}\|\|\tilde{x}(t_0)\| + \int_{t_0}^t \|e^{-H(t-\tau)}\|\|\nu^x(\tau)\|d\tau \\ &\le \alpha e^{-\beta(t-t_0)}\|\tilde{x}(t_0)\| + \alpha(\varpi_v + \varpi_\theta),\end{aligned} \tag{33}$$

where $\varpi_v = \int_{t_0}^t e^{-\beta(t-\tau)}\|\tilde{v}(\tau)\|d\tau$ and $\varpi_\theta = l_c v_0^+ \int_{t_0}^t e^{-\beta(t-\tau)}\|\tilde{\theta}(\tau)\|d\tau$. Note that $t - \tau \ge 0$. Then, using (32), ϖ_v satisfies

$$\varpi_v \le \alpha_1\|\tilde{v}(t_0)\|e^{\beta_1 t_0 - \beta t}\int_{t_0}^t e^{(\beta-\beta_1)\tau}d\tau. \tag{34}$$

If $\beta = \beta_1$, $\varpi_v \le \alpha_1\|\tilde{v}(t_0)\|(t-t_0)e^{-\beta(t-t_0)}$, otherwise $\varpi_v \le \alpha_1\|\tilde{v}(t_0)\|(\beta-\beta_1)^{-1}(e^{-\beta_1(t-t_0)} - e^{-\beta(t-t_0)})$.

Similarly, if $\beta = \beta_2$, $\varpi_\theta \le \alpha_2\|\tilde{\theta}(t_0)\|(t-t_0)e^{-\beta(t-t_0)}$, otherwise $\varpi_\theta \le \alpha_2\|\tilde{\theta}(t_0)\|(\beta-\beta_2)^{-1}(e^{-\beta_2(t-t_0)} - e^{-\beta(t-t_0)})$.

Therefore, it follows from (33) that $\|\tilde{x}(t)\| \to 0$ exponentially as $t \to \infty$. In the same way, one can prove that $\|\tilde{y}(t)\| \to 0$ exponentially as $t \to \infty$.

Hence, system (30) is globally exponentially stable and $\|\hat{x}_i(t) - x_0(t)\| \to 0$ and $\|\hat{y}_i(t) - y_0(t)\| \to 0$ exponentially as $t \to \infty$. The proof is thus completed. ∎

Remark 3.1: Assumption [A3] ensures that each node in the digraph $\bar{\mathcal{G}}$ is reachable from node 0, and thus the information associated with the leader can be properly estimated with observer (19)–(22). The design of observer (21) and (22) for vehicle i follows from [33], which requires $[\hat{\theta}_j\ \hat{v}_j]^\top$ and its derivative $[\dot{\hat{\theta}}_j\ \dot{\hat{v}}_j]^\top$ from its neighbors. In fact, the derivative can be calculated by numerical differentiation. It is noted that the time delay of intervehicle communication is assumed to be negligible in this paper.

B. Velocity Controller Design

To satisfy the velocity constraints (2) and (3), the velocity controller in the form of (6) is designed as follows:

$$v_i = \mathrm{sat}(\hat{v}_i, v_r^+, v_r^-) + \frac{k_1\tilde{x}_{ei}}{\sqrt{1+\tilde{x}_{ei}^2+\tilde{y}_{ei}^2}}, \tag{35}$$

$$\begin{aligned}\omega_i &= \mathrm{sat}(\dot{\hat{\theta}}_i, \omega_r^+, -\omega_r^+) + \frac{k_3\sin\frac{\tilde{\theta}_{ei}}{2}}{\sqrt{1+\tilde{x}_{ei}^2+\tilde{y}_{ei}^2}} \\ &+ \frac{k_2\mathrm{sat}(\hat{v}_i, v_r^+, v_r^-)(\tilde{y}_{ei}\cos\frac{\tilde{\theta}_{ei}}{2} - \tilde{x}_{ei}\sin\frac{\tilde{\theta}_{ei}}{2})}{\sqrt{1+\tilde{x}_{ei}^2+\tilde{y}_{ei}^2}},\end{aligned} \tag{36}$$

where $\tilde{x}_{ei}$, $\tilde{y}_{ei}$, and $\tilde{\theta}_{ei}$ are obtained from (18) by using the following coordinate transformation:

$$[\tilde{x}_{ei}\ \tilde{y}_{ei}]^\top = R(\theta_i)[\hat{e}_i^x\ \hat{e}_i^y]^\top,\ \tilde{\theta}_{ei} = \hat{e}_i^\theta. \tag{37}$$

Function $z = \mathrm{sat}(a,b,c) : \mathbb{R}^3 \mapsto \mathbb{R}$ is defined as $z = a$, if $c \le a \le b$; $z = b$, if $a > b$ and $z = c$, if $a < c$. Moreover, k_1, k_2, and k_3 are positive constants satisfying

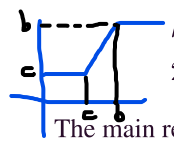

$$\begin{aligned}&k_1 \le \min(v_{\max} - v_r^+,\ v_r^- - v_{\min}), \\ &2k_2 v_r^+ + k_3 \le \omega_{\max} - \omega_r^+.\end{aligned} \tag{38}$$

The main result of this paper is summarized as follows.

Theorem 3.1: Consider the digraph $\bar{\mathcal{G}}$, and the closed-loop system consisting of N error systems (17) and the distributed dynamic control law (19)–(22) and (35)–(36). Under assumptions [A1]–[A3], the design parameters k_1, k_2, and k_3 can always be tuned such that the closed-loop system is uniformly asymptotically stable for any initial states $[x_{ei}(t_0)\ y_{ei}(t_0)]^\top \in \mathbb{R}^2$ and $\theta_{ei}(t_0) \in (-2\pi,\ 2\pi)$, $\forall t_0 \ge 0$, while the velocity constraints (2) and (3) are satisfied for all $t \ge t_0$. Equivalently, the leader–follower formation control problem is solved by the distributed dynamic control law (19)–(22) and (35)–(36) under assumptions [A1]–[A3].

Proof: Based on (23), define

$$[\bar{x}_i\ \bar{y}_i]^\top = R(\theta_i)[\tilde{x}_i\ \tilde{y}_i]^\top, \quad \bar{\theta}_i = -\tilde{\theta}_i, \tag{39}$$

$$\bar{v}_i = \mathrm{sat}(\hat{v}_i, v_r^+, v_r^-) - v_0, \quad \bar{\omega}_i = \mathrm{sat}(\dot{\hat{\theta}}_i, \omega_r^+, -\omega_r^+) - \omega_0. \tag{40}$$

Thus, $\bar{x}_i = x_{ei} - \tilde{x}_{ei}$, $\bar{y}_i = x_{ei} - \tilde{y}_{ei}$, and $\bar{\theta}_i = \theta_{ei} - \tilde{\theta}_{ei}$. Let

$$\chi_i = [x_{ei}\ y_{ei}\ \theta_{ei}]^\top, \quad \xi_i = [\bar{x}_i\ \bar{y}_i\ \bar{\theta}_i\ \bar{v}_i\ \bar{\omega}_i]^\top. \tag{41}$$

Using (37)–(39), system (17) can be written in the form of

$$\dot{\chi}_i = f(\chi_i, \gamma(t)) + g(\chi_i, \xi_i, \gamma(t)), \tag{42}$$

with $\gamma(t) := [v_0(t)\ \omega_0(t)]^\top$ and

$$f(\chi_i, \gamma(t)) = \begin{bmatrix}\omega_{ei}y_{ei} - v_{ei} + v_0\cos\theta_{ei} \\ -\omega_{ei}x_{ei} + v_0\sin\theta_{ei} \\ \omega_0 - \omega_{ei}\end{bmatrix},$$

$$g(\chi_i, \xi_i, \gamma(t)) = \begin{bmatrix}y_{ei}(\omega_i - \omega_{ei}) - (v_i - v_{ei}) \\ -x_{ei}(\omega_i - \omega_{ei}) \\ -(\omega_i - \omega_{ei})\end{bmatrix},$$

where

$$\omega_{ei} = \omega_0 + \frac{k_2 v_0 (y_{ei}\cos\frac{\theta_{ei}}{2} - x_{ei}\sin\frac{\theta_{ei}}{2}) + k_3 \sin\frac{\theta_{ei}}{2}}{\sqrt{1+x_{ei}^2+y_{ei}^2}}, \tag{43}$$

$$v_{ei} = v_0 + \frac{k_1 x_{ei}}{\sqrt{1+x_{ei}^2+y_{ei}^2}}. \tag{44}$$

Then, define p_{ei}, $\bar{p}_{ei}$, and q_{ei} in (45), which is shown at the bottom of the page. Thus, $\omega_i - \omega_{ei}$ and $v_i - v_{ei}$ can be expressed as (46) and (47), respectively, which are shown at the bottom of the page. Note that $\frac{\sin q}{q} = \int_0^1 \cos(qs)ds$ is a smooth function and $|\frac{\sin q}{q}| \le 1$. It follows from (43)–(47) that $f(\chi_i, \gamma(t))$ and $g(\chi_i, \xi_i, \gamma(t))$ are continuous in their augments, $f(\chi_i, \gamma(t))$ is locally Lipschitz on χ_i uniformly on γ, and $g(\chi_i, \xi_i, \gamma(t))$ is locally Lipschitz on (χ_i, ξ_i) uniformly on γ. In what follows, Corollary 2.1 will be used to prove Theorem 3.1.

First, it will show that system $\dot{\chi}_i = f(\chi_i, \gamma(t))$ is uniformly asymptotically stable at $\chi_i = 0$ for all $\chi_i \in \mathcal{X}$ with

$$\mathcal{X} = \{(x, y, \theta) | x \in \mathbb{R},\ y \in \mathbb{R},\ \theta \in (-2\pi,\ 2\pi)\}. \tag{48}$$

Consider a Lyapunov function candidate $V_i(t, \chi_i) : \mathbb{R}_{\ge 0} \times \mathcal{X} \mapsto \mathbb{R}_{\ge 0}$ as

$$V_i(t, \chi_i) = \frac{k_2}{2}\left(\sqrt{1+x_{ei}^2+y_{ei}^2} - 1\right) + 8\sin^2\frac{\theta_{ei}}{4}, \tag{49}$$

which is positive-definite and decrescent, and $V_i(t, \chi_i) \to \infty$ as $\|[x_{ei}\ y_{ei}]^\intercal\| \to \infty$. Taking the time derivative of $V_i(t, \chi_i)$ along the trajectories of system $\dot{\chi}_i = f(\chi_i, \gamma(t))$ yields

$$\begin{aligned}
\dot{V}_i(t, \chi_i) &= \frac{k_2(x_{ei}\dot{x}_{ei} + y_{ei}\dot{y}_{ei})}{\sqrt{1+x_{ei}^2+y_{ei}^2}} + 2\dot{\theta}_{ei}\sin\frac{\theta_{ei}}{2} \\
&= \frac{-k_1 k_2 x_{ei}^2}{1+x_{ei}^2+y_{ei}^2} - \frac{k_2 v_0 (x_{ei}(1-\cos\theta_{ei}) - y_{ei}\sin\theta_{ei})}{\sqrt{1+x_{ei}^2+y_{ei}^2}} \\
&\quad - \frac{2k_2 v_0 \sin\frac{\theta_{ei}}{2}(y_{ei}\cos\frac{\theta_{ei}}{2} - x_{ei}\sin\frac{\theta_{ei}}{2})}{\sqrt{1+x_{ei}^2+y_{ei}^2}} - \frac{2k_3\sin^2\frac{\theta_{ei}}{2}}{\sqrt{1+x_{ei}^2+y_{ei}^2}} \\
&= \frac{-k_1 k_2 x_{ei}^2}{1+x_{ei}^2+y_{ei}^2} - \frac{k_2 v_0 (2x_{ei}\sin^2\frac{\theta_{ei}}{2} - 2y_{ei}\sin\frac{\theta_{ei}}{2}\cos\frac{\theta_{ei}}{2})}{\sqrt{1+x_{ei}^2+y_{ei}^2}} \\
&\quad - \frac{2k_2 v_0 \sin\frac{\theta_{ei}}{2}(y_{ei}\cos\frac{\theta_{ei}}{2} - x_{ei}\sin\frac{\theta_{ei}}{2})}{\sqrt{1+x_{ei}^2+y_{ei}^2}} - \frac{2k_3\sin^2\frac{\theta_{ei}}{2}}{\sqrt{1+x_{ei}^2+y_{ei}^2}} \\
&= -\frac{k_1 k_2 x_{ei}^2}{1+x_{ei}^2+y_{ei}^2} - \frac{2k_3\sin^2\frac{\theta_{ei}}{2}}{\sqrt{1+x_{ei}^2+y_{ei}^2}} \le 0.
\end{aligned} \tag{50}$$

Thus, $V_i(t, \chi_i)$ is nonincreasing in t and bounded, which implies that $\lim_{t\to\infty}\int_0^t \dot{V}_i(\tau, \chi_i)d\tau$ exists and is finite. It follows from $V_i(t, \chi_i) \le V_i(0, \chi_i(0))$ that x_{ei} and y_{ei} are bounded, which implies that $\dot{x}_{ei}$, $\dot{y}_{ei}$, and $\dot{\theta}_{ei}$ are also bounded. Then, $\ddot{V}_i(t, \chi_i)$ is bounded with respect to x_{ei}, y_{ei}, and θ_{ei}, and is bounded with respect to t. Thus, $\dot{V}_i(t, \chi_i)$ is uniformly continuous in t. It follows from Barbalat's Lemma that $\lim_{t\to\infty} x_{ei}^2 = 0$ and $\lim_{t\to\infty}\sin^2\frac{\theta_{ei}}{2} = 0$, which yields

$$\lim_{t\to\infty} x_{ei} = 0,\ \lim_{t\to\infty}\theta_{ei} = 0. \tag{51}$$

Next, the extended Barbalat's Lemma [11, Lemma A.14] will be employed to prove that $y_{ei} \to 0$ when $x_{ei},\ \theta_{ei} \to 0$.

Define a function $\mu(t) = y_{ei}\sin\theta_{ei}$. Since $\lim_{t\to\infty}\theta_{ei} = 0$ and y_{ei} is bounded, $\lim_{t\to\infty}\mu(t) = 0$. Taking the time derivative of $\mu(t)$ along the trajectories of system $\dot{\chi}_i = f(\chi_i, \gamma(t))$ yields

$$\dot{\mu}(t) = \dot{y}_{ei}\sin\theta_{ei} + \dot{\theta}_{ei}y_{ei}\cos\theta_{ei} = h_1(t) + h_2(t), \tag{52}$$

where $h_1(t) = -k_2 v_0 y_{ei}^2 \cos\theta_{ei}\cos\frac{\theta_{ei}}{2}/\sqrt{p_{ei}}$ and $h_2(t) = \dot{y}_{ei}\sin\theta_{ei} + y_{ei}\cos\theta_{ei}(k_2 v_0 x_{ei}\sin\frac{\theta_{ei}}{2} - k_3\sin\frac{\theta_{ei}}{2})/\sqrt{p_{ei}}$.

Since x_{ei}, y_{ei}, $\dot{x}_{ei}$, $\dot{y}_{ei}$, and $\dot{\theta}_{ei}$ are bounded, and v_r and ω_r satisfy assumption [A1], then $\dot{h}_1(t)$ is bounded. Thus, $h_1(t)$ is uniformly continuous in t. It follows from (51) that $\lim_{t\to\infty} h_2(t) = 0$. By the extended Barbalat's Lemma, $\lim_{t\to\infty} h_1(t) = 0$, which together with assumption [A1] yields

$$\lim_{t\to\infty} y_{ei} = 0. \tag{53}$$

Hence, system $\dot{\chi}_i = f(\chi_i, \gamma(t))$ is uniformly asymptotically stable for $\chi \in \mathcal{X}$. It is noticed that $V_i(t, \chi_i)$ satisfies (10) for any $\chi \in \mathcal{X}$. It follows from (50) that $\dot{V}_i(t, \chi_i)$ satisfies (11) for any $\chi \in \mathcal{X}$. Moveover, since

$$\left\|\frac{\partial V_i}{\partial \chi_i}\right\| = \sqrt{\frac{k_2^2(x_{ei}^2+y_{ei}^2)}{1+x_{ei}^2+y_{ei}^2} + 4\sin^2\frac{\theta_{ei}}{2}} < \sqrt{k_2^2+4}, \tag{54}$$

there exist constants $c_{1i} > 2\sqrt{k_2^2+4}/k_2$, $\zeta_i > k_2/(c_{1i}k_2 - 2\sqrt{k_2^2+4})$, and $c_{2i} \ge \sqrt{k_2^2+4}$, such that (12) holds for all $\chi_i \in \{\chi_i \in \mathcal{X} |\ \|\chi_i\| \ge \zeta_i\}$, and (13) holds for all $\chi_i \in \{\chi_i \in \mathcal{X} |\ \|\chi_i\| \le \zeta_i\}$. Thus, condition (i) in Corollary 2.1 is satisfied.

Second, under assumption [A3], Lemma 3.1 holds. For any $\bar{\theta}_i(t_0)$, $\bar{\theta}_i(t) \to 0$ exponentially as $t \to \infty$. Since $\|[\bar{x}_i\ \bar{y}_i]^\intercal\|$

$$p_{ei} = 1+x_{ei}^2+y_{ei}^2,\ \bar{p}_{ei} = 1+(x_{ei}-\bar{x}_i)^2+(y_{ei}-\bar{y}_i)^2,\ q_{ei} = k_2 v_0\left(y_{ei}\cos\frac{\theta_{ei}}{2} - x_{ei}\sin\frac{\theta_{ei}}{2}\right) + k_3\sin\frac{\theta_{ei}}{2}, \tag{45}$$

$$\begin{aligned}
\omega_i - \omega_{ei} &= \bar{x}_i\left(\frac{k_2 v_0 \sin(\frac{\theta_{ei}}{2} - \frac{\bar{\theta}_i}{2})}{\sqrt{\bar{p}_{ei}}} - \frac{(\bar{x}_i - 2x_{ei})q_{ei}}{\bar{p}_{ei}\sqrt{p_{ei}} + p_{ei}\sqrt{\bar{p}_{ei}}}\right) + \bar{y}_i\left(\frac{-k_2 v_0\cos(\frac{\theta_{ei}}{2} - \frac{\bar{\theta}_i}{2})}{\sqrt{\bar{p}_{ei}}} + \frac{(\bar{y}_i - 2y_{ei})q_{ei}}{\bar{p}_{ei}\sqrt{p_{ei}} + p_{ei}\sqrt{\bar{p}_{ei}}}\right) + \bar{\omega}_i \\
&\quad + \bar{\theta}_i\left(\frac{k_2 v_0 \sin\frac{\bar{\theta}_i}{2}}{\bar{\theta}_i}\frac{(x_{ei}\cos\frac{\theta_{ei}}{2} + y_{ei}\sin\frac{\theta_{ei}}{2})}{\sqrt{\bar{p}_{ei}}} - \frac{2\sin^2\frac{\bar{\theta}_i}{4}}{\bar{\theta}_i}\frac{q_{ei}}{\sqrt{\bar{p}_{ei}}}\right) + \bar{v}_i\left(\frac{k_2((y_{ei}-\bar{y}_i)\cos\frac{\theta_{ei}-\bar{\theta}_i}{2} - (x_{ei}-\bar{x}_i)\sin\frac{\theta_{ei}-\bar{\theta}_i}{2})}{\sqrt{\bar{p}_{ei}}}\right),
\end{aligned} \tag{46}$$

$$v_i - v_{ei} = \bar{v}_i - \bar{x}_i k_1\left(\frac{1}{\sqrt{\bar{p}_{ei}}} + \frac{x_{ei}(\bar{x}_i - 2x_{ei})}{\bar{p}_{ei}\sqrt{p_{ei}} + p_{ei}\sqrt{\bar{p}_{ei}}}\right) - \bar{y}_i k_1\left(\frac{x_{ei}(\bar{y}_i - 2y_{ei})}{\bar{p}_{ei}\sqrt{p_{ei}} + p_{ei}\sqrt{\bar{p}_{ei}}}\right), \tag{47}$$

$= \|[\tilde{x}_i\ \tilde{y}_i]^\top\|$ holds from (39), and system (30) is globally exponentially stable, $\|[\bar{x}_i(t)\ \bar{y}_i(t)]^\top\| \to 0$ exponentially as $t\to\infty$ for any $[\bar{x}_i(t_0)\ \bar{y}_i(t_0)]^\top$. For $v_0(t)$ satisfying assumption [A1] and any $\hat{v}_i(t)$, $|\bar{v}_i(t)| = |\operatorname{sat}(\hat{v}_i(t), v_r^+, v_r^-) - v_0(t)| \le |\hat{v}_i(t) - v_0(t)|$. By Lemma 3.1, $|\bar{v}_i(t)| \to 0$ exponentially as $t\to\infty$ and so does $|\bar{\omega}_i(t)|$. Hence, there exist positive constants k and ς, such that for any $\xi_i(t_0)$, $\|\xi_i(t)\| \le k\|\xi_i(t_0)\|e^{-\varsigma(t-t_0)}$, which satisfies condition (ii) in Corollary 2.1.

Third, by using the following inequalities:

$$\begin{aligned}&|x_{ei}|/\sqrt{p_{ei}} < 1,\ |y_{ei}|/\sqrt{p_{ei}} < 1,\ (|x_{ei} - \bar{x}_i|)/\sqrt{p_{ei}} < 1,\\ &(|y_{ei} - \bar{y}_i|)/\sqrt{p_{ei}} < 1,\ |\bar{x}_i|/\sqrt{p_{ei}} \le |\bar{x}_i|,\ |\bar{y}_i|/\sqrt{p_{ei}} \le |\bar{y}_i|,\\ &|x_{ei}|/\sqrt{p_{ei}} \le \sqrt{1+|\bar{x}_i|^2},\ |y_{ei}|/\sqrt{p_{ei}} \le \sqrt{1+|\bar{y}_i|^2}, \end{aligned} \tag{55}$$

one can obtain inequalities (56) and (57), which are shown at the bottom of the page, from (46) and (47). Noting

$$\begin{aligned}\|g(\chi_i,\xi_i,\gamma(t))\| &\le |(v_i - v_{ei}) - y_{ei}(\omega_i - \omega_{ei})| + (1+|x_{ei}|)\\ &\times|\omega_i - \omega_{ei}| \le |v_i - v_{ei}| + (1+|x_{ei}|+|y_{ei}|)|\omega_i - \omega_{ei}|,\end{aligned} \tag{58}$$

it follows from (56) and (57) that $\|g(\chi_i,\xi_i,\gamma(t))\|$ satisfies

$$\|g(\chi_i,\xi_i,\gamma(t))\| \le \|\xi_i\|\Theta_1(\|\xi_i\|) + \|\xi_i\|\|\chi_i\|\Theta_2(\|\xi_i\|), \tag{59}$$

where $\Theta_1,\ \Theta_2 : \mathbb{R}_{\ge 0} \mapsto \mathbb{R}_{\ge 0}$ are continuous functions in $\|\xi_i\|$. This satisfies condition (iii) in Corollary 2.1.

Thus, by Corollary 2.1, system (42) is uniformly asymptotically stable for $\chi \in \mathcal{X}$.

Finally, since v_0 and ω_0 satisfy assumption [A1] and $\tilde{x}_{ei}/\sqrt{1+\tilde{x}_{ei}^2+\tilde{y}_{ei}^2}$, $\tilde{y}_{ei}/\sqrt{1+\tilde{x}_{ei}^2+\tilde{y}_{ei}^2} \in (-1,1)$, then k_1, k_2, and k_3 can be tuned in accordance with (38) such that velocity constraints (2) and (3) are always satisfied. The proof is thus completed. ∎

Remark 3.2: A conservative method to tune the design parameters k_1, k_2, and k_3 is given in (38), such that the velocity constraints (2) and (3) are always satisfied. If the bounds v_0^-, v_0^+ and ω_0^-, ω_0^+ are assumed to be known, v_r^-, v_r^+, and ω_r^+ in (38) can be replaced with v_0^-, v_0^+, and ω_0^+, such that k_1, k_2, and k_3 may be selected larger. For vehicles with linear velocity saturation instead of constraint (2) [20], [21], i.e., $v_i \in [-v_{\max},\ v_{\max}]$, $i = 0,1,\ldots,N$, the parameters k_1, k_2, and k_3 in (35)–(36) can also be tuned such that the linear velocity saturation and constraint (3) are satisfied, and vehicle formation can be achieved if $v_0(t)$ does not converge to 0.

Remark 3.3: In [27], a distributed formation control law was proposed and the velocity constraint (2) can be satisfied. This control law design required each follower vehicle to measure the relative positions to its neighbors from a static sensing digraph and to have access to the real-time information of the leader, $\theta_0(t), \omega_0(t), v_0(t)$, and $\dot{v}_0(t)$ from communication. This result was extended in [28] to the case, where the sensing digraph is time-varying, and $\theta_0(t)$, $\omega_0(t)$, $v_0(t)$ are known to all followers. In this paper, the velocity constraint (3) is additionally taken into account. More importantly, any real-time information of the leader, including $\theta_0(t)$, $\omega_0(t)$, $v_0(t)$, and $\dot{v}_0(t)$, is not required to be known to all followers. Each vehicle only uses the information of itself and its neighbors in the proposed control law (19)–(22) and (35)–(36).

Remark 3.4: It can be observed from (4) and (7) that the achieved vehicle formation is defined in inertial frame. For vehicle formation defined in the local Frenet–Serret frame of the leader, the tracking errors $[x_{ei}\ y_{ei}\ \theta_{ei}]^\top$ in (16) can be redefined as

$$\begin{bmatrix} x_{ei}\\ y_{ei}\end{bmatrix} = R(\theta_i)\begin{bmatrix} x_0 - x_i\\ y_0 - y_i\end{bmatrix} + \begin{bmatrix} h_{i0}^x\\ h_{i0}^y\end{bmatrix},\quad \theta_{ei} = \theta_0 - \theta_i, \tag{60}$$

where $\boldsymbol{h}_{i0} := [h_{i0}^x\ h_{i0}^y]^\top$ is the desired relative position between vehicle i and the leader. Let $\boldsymbol{h}_{ij} := [h_{ij}^x\ h_{ij}^y]^\top$, $j\in\mathcal{N}_i$, denote the desired relative position between vehicles i and j in the local frame of vehicle i. In this case, $[d_{i0}^x\ d_{i0}^y]^\top$ in (4) and (18), and $[d_{ij}^x\ d_{ij}^y]^\top$ in (19) and (20) can be replaced, respectively, with

$$[d_{i0}^x\ d_{i0}^y]^\top = R(-\theta_i)\boldsymbol{h}_{i0},\ [d_{ij}^x\ d_{ij}^y]^\top = R(-\theta_i)\boldsymbol{h}_{ij}. \tag{61}$$

Then, the design of observer (19) and (20) is modified as

$$\begin{aligned}\dot{\hat{e}}_i^x &= \hat{v}_i\cos\hat{\theta}_i - v_i\cos\theta_i - \omega_i d_{i0}^y\\ &\quad + \sum_{j\in\mathcal{N}_i} a_{ij}\left((\hat{e}_j^x - \hat{e}_i^x) + (x_j - x_i) + d_{ij}^x\right),\end{aligned} \tag{62}$$

$$\begin{aligned}\dot{\hat{e}}_i^y &= \hat{v}_i\sin\hat{\theta}_i - v_i\sin\theta_i + \omega_i d_{i0}^x\\ &\quad + \sum_{j\in\mathcal{N}_i} a_{ij}\left((\hat{e}_j^y - \hat{e}_i^y) + (y_j - y_i) + d_{ij}^y\right).\end{aligned} \tag{63}$$

Using $[\dot{d}_{i0}^x\ \dot{d}_{i0}^y]^\top = \omega_i S R(-\theta_i)[h_{i0}^x\ h_{i0}^y]^\top = \omega_i S[d_{i0}^x\ d_{i0}^y]^\top$ with $S = \begin{bmatrix} 0 & 1\\ -1 & 0\end{bmatrix}$ and $[d_{ij}^x\ d_{ij}^y]^\top = [d_{i0}^x - d_{j0}^x\ d_{i0}^y - d_{j0}^y]^\top$, one can obtain system (30). In this case, Lemma 3.1 still holds. Thus, the dynamic control law consisting of (21)–(22), (35)–(36), and (62)–(63) can be applied to this case if $\boldsymbol{h}_{i0}$ is known.

$$\begin{aligned}|\omega_i - \omega_{ei}| &\le |\bar{x}_i|\left(k_2v_0^+ + \frac{(|\bar{x}_i|+2|x_{ei}|)(k_2v_0^+(|y_{ei}|+|x_{ei}|)+k_3)}{p_{ei}\sqrt{p_{ei}}}\right) + |\bar{y}_i|\left(k_2v_0^+ + \frac{(|\bar{y}_i|+2|y_{ei}|)(k_2v_0^+(|y_{ei}|+|x_{ei}|)+k_3)}{p_{ei}\sqrt{p_{ei}}}\right)\\ &\quad + |\bar{\theta}_i|\left(\frac{k_2v_0^+(|y_{ei}|+|x_{ei}|)}{2\sqrt{p_{ei}}} + \frac{k_2v_0^+(|y_{ei}|+|x_{ei}|)+k_3}{2\sqrt{p_{ei}}}\right) + |\bar{v}_i|\left(\frac{k_2(|y_{ei}-\bar{y}_i|+|x_{ei}-\bar{x}_i|)}{\sqrt{p_{ei}}}\right) + |\bar{\omega}_i|\\ &\le \|\xi_i\|(2k_2v_0^+ + 2(2k_2v_0^+ + k_3)(\|\xi_i\|+2) + 2k_2v_0^+\sqrt{1+\|\xi_i\|^2} + \frac{k_3}{2} + 2k_2 + 1),\end{aligned} \tag{56}$$

$$\begin{aligned}|v_i - v_{ei}| &\le k_1|\bar{x}_i|\left(1 + \frac{|x_{ei}\bar{x}_i| + 2|x_{ei}|^2}{p_{ei}\sqrt{p_{ei}}}\right) + k_1|\bar{y}_i|\left(\frac{|x_{ei}\bar{y}_i| + 2|x_{ei}y_{ei}|}{p_{ei}\sqrt{p_{ei}}}\right) + |\bar{v}_i|\\ &\le k_1|\bar{x}_i|(|\bar{x}_i|+3) + k_1|\bar{y}_i|(|\bar{y}_i|+2) + |\bar{v}_i| \le \|\xi_i\|(k_1(2\|\xi_i\|+5)+1),\end{aligned} \tag{57}$$

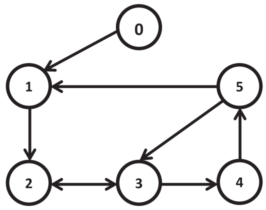

Fig. 1. Digraph $\bar{\mathcal{G}}$ describing the network among mobile robots.

Remark 3.5: To obtain the proposed control law in real time, each follower vehicle is required to compute the real-time internal state $[\hat{e}_i\ \hat{\theta}_i\ \hat{v}_i\ \dot{\hat{\theta}}_i\ \dot{\hat{v}}_i]^{\mathrm{T}}$ of observer (19)–(22) by iteration and constant memory space is thus needed. It should be noted that no matrix operation is required in (19)–(22) and (35)–(36). Instead, only scalar operation is used in the real-time computation of each follower. To be specific, real-time computation of follower vehicle i includes a small number of arithmetic operations ($12|\mathcal{N}_i| + 18$ additions, 20 multiplications, 3 divisions, and 1 square root) and elementary function operations (3 sine functions and 3 cosine functions), where $|\mathcal{N}_i|$ is the number of neighbors of vehicle i.

IV. Illustrative Example

In this section, a practical example adopted from [27] will be considered, where five nonholonomic mobile robots with kinematics (1) are required to follow a leader robot and maintain a rectangle formation. It is noted that system (1) can be used to describe not only a nonholonomic mobile robot [2], [11], [32], but also the simplified model of a UAV equipped with standard autopilots or a fixed-wing UAV, see [2], [8], and references therein. By default, the values of variables are in SI units. For convenience, the units are omitted in the following.

Consider a leader robot (labeled 0) and five follower robots (labeled 1–5) with kinematics (1). The velocity constraints are given as $v_i \in [3-1.8\sqrt{2},\ 3+1.8\sqrt{2}]$ and $\omega_i \in [-1.2,\ 1.2]$. The bounds of the group reference velocities are $v_r^+ = 4.5$, $v_r^- = 2$, and $\omega_r^+ = 0.3$. The linear velocity and the angular velocity of the leader robot are given as $v_0(t) = 3.25 - 0.25\cos 0.24t$ and $\omega_0(t) = 0.1\cos 0.2t$, which satisfy assumptions [A1] and [A2]. Based on (38), tune the design parameters $k_1 = 1.5$, $k_2 = 0.05$, and $k_3 = 0.45$.

The desired geometric pattern is a rectangle. For follower robots, the desired relative positions to the leader are given by $[d_{10}^x\ d_{20}^x\ d_{30}^x\ d_{40}^x\ d_{50}^x]^{\mathrm{T}} = [-30\ -30\ 0\ 30\ 30]^{\mathrm{T}}$ and $[d_{10}^y\ d_{20}^y\ d_{30}^y\ d_{40}^y\ d_{50}^y]^{\mathrm{T}} = [0\ -30\ -30\ -30\ 0]^{\mathrm{T}}$. The digraph $\bar{\mathcal{G}}$ is shown in Fig. 1, which satisfies assumption [A3].

In this example, the initial states $\hat{e}_i^x(0)$, $\hat{e}_i^y(0)$, $\hat{\theta}_i(0)$, $\hat{v}_i(0)$, $\dot{\hat{\theta}}_i(0)$, and $\dot{\hat{v}}_i(0)$ are listed in Table I. Note that they can be randomly chosen. For the leader robot, $[\hat{e}_0(0)\ \hat{\theta}_0(0)\ \hat{v}_0(0)\ \dot{\hat{\theta}}_0(0)\ \dot{\hat{v}}_0(0)]^{\mathrm{T}} = [0\ \theta_0(0)\ v_0(0)\ \omega_0(0)\ \dot{v}_0(0)]^{\mathrm{T}}$. The initial states of all robots, $[x_i(0)\ y_i(0)\ \theta_i(0)]^{\mathrm{T}}$, $i = 0, 1, \ldots, N$, are the same as that in [27]. Then, apply the distributed control law (19)–(22) and (35)–(36) to each follower robot.

TABLE I
Initial States of Variables in (19)–(22)

Label	$[\hat{e}_i^x(0)\ \hat{e}_i^y(0)]^{\mathrm{T}}$	$\hat{\theta}_i(0)$	$\hat{v}_i(0)$	$\dot{\hat{\theta}}_i(0)$	$\dot{\hat{v}}_i(0)$
1	$[-24.49\ 12.86]^{\mathrm{T}}$	π	3	0.1	0.15
2	$[-5.66\ -10.55]^{\mathrm{T}}$	$5\pi/6$	3.5	-0.2	-0.21
3	$[-2.49\ -17.61]^{\mathrm{T}}$	0	4.5	0.25	-0.18
4	$[29.72\ 22.81]^{\mathrm{T}}$	$-2\pi/3$	2.5	0.25	0.13
5	$[-30.00\ -28.00]^{\mathrm{T}}$	0	2	-0.15	0.16

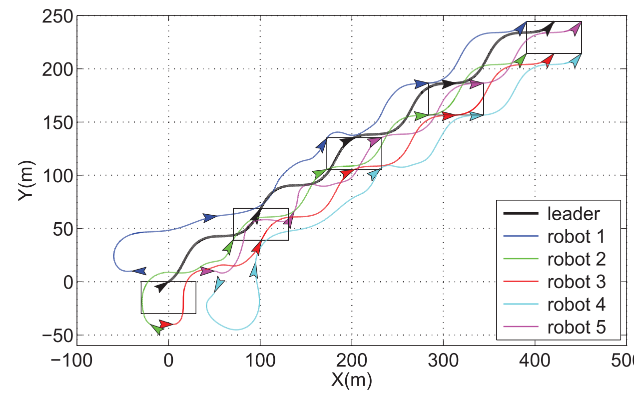

Fig. 2. Trajectories of all mobile robots.

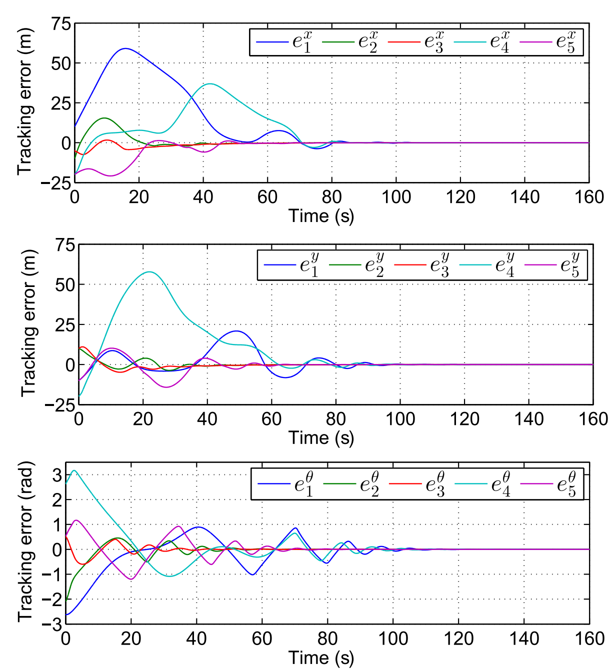

Fig. 3. Formation tracking errors of each follower robot.

Fig. 2 presents the trajectories of all mobile robots during 0–160 s, which shows that robots converge to the desired formation. Fig. 3 shows that the formation tracking errors $e_i^x(t)$, $e_i^y(t)$, and $e_i^\theta(t)$ converge to 0, and the objective (7) is achieved. Fig. 4 shows that all velocities $v_i(t)$ and $\omega_i(t)$ always stay in the constrained ranges, which indicates the velocity constraints (2) and (3) are satisfied. These results verify the effectiveness of the proposed control law.

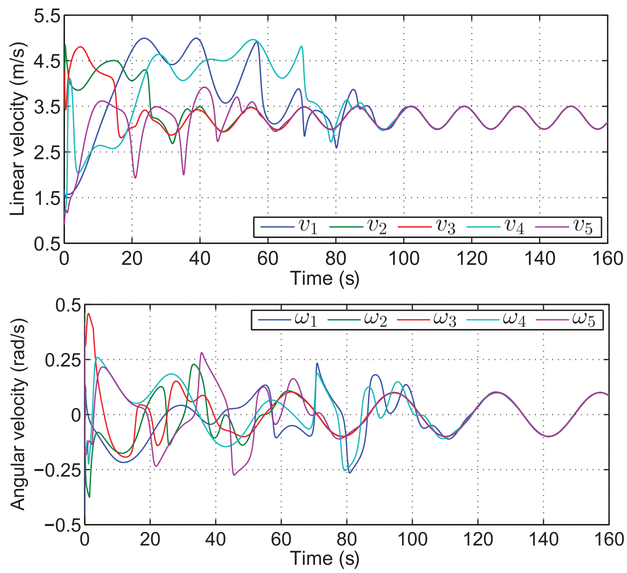

Fig. 4. Velocities of each follower robot.

V. Conclusion

A distributed formation control law has been proposed for networked nonholonomic vehicles subject to velocity constraints. Particularly, the linear velocity of each vehicle is constrained to lie between two positive constants. With the proposed control law, the leader–follower formation can be achieved in the scenario, where absolute position measurements are not available and each follower vehicle only has access to the information of its neighboring vehicles in a network modeled by a directed graph.

Based on the obtained result, it is of interest to further study the formation control of networked nonholonomic vehicles by considering more practical issues. First, the static network will be extended to the time-varying one. Investigating connectivity preservation and collision avoidance within a state-dependent network will also be interesting. Second, the presence of unknown disturbances and uncertainties will be considered. Third, the time delay intervehicle information exchange will be taken into account.

Appendix

Due to page limitations, only a sketch of proof of Lemma 2.1 is presented. The proof follows from the proof of Theorem 1 and Theorem 2 in [29] by showing that i) the solution of (8) is globally uniformly bounded; ii) system (8) is uniformly stable; and iii) system (8) is uniformly asymptotically stable.

Denote $\dot{\vartheta}_{(\#)}(\cdot)$ as the time derivative of function $\vartheta(\cdot)$ along the solution of the differential equation labeled $(\#)$. Different from [29], Lemma 2.1 does not require that $f(\chi, \gamma(t))$ is continuously differentiable and $\dot{V}_{(9)}(t, \chi)$ is negative definite. However, to show (i) and (ii), one can still follow the proof of Theorem 1 in [29]. To prove (iii), at first, the smooth converse Lyapunov theorem [31, Theorem 2.9] is utilized to find a smooth Lyapunov function $\mathcal{V}(\chi)$ with respect to the origin of the nominal system (9). From Definition 2.6 in [31], $\dot{\mathcal{V}}_{(9)}(\chi)$ is negative definite and $\mathcal{V}(\chi) \leq \overline{\alpha}(\chi)$, $\overline{\alpha} \in \mathcal{K}_{\infty}$. It follows from (i) and the continuity of $\frac{\partial \mathcal{V}(\chi)}{\partial \chi}$ that $\|\frac{\partial \mathcal{V}(\chi)}{\partial \chi}\|$ is uniformly bounded. The remaining proof for (iii) can be shown by following the proof of Theorem 2 in [29].

Acknowledgment

The authors would like to thank the Associate Editor and the Anonymous Reviewers for their valuable comments.

References

[1] J. A. Fax and R. M. Murray, "Information flow and cooperative control of vehicle formations," *IEEE Trans. Autom. Control*, vol. 49, no. 9, pp. 1465–1476, Sep. 2004.

[2] Z. Qu, *Cooperative Control of Dynamical Systems: Applications to Autonomous Vehicles*. Berlin, Germany: Springer-Verlag, 2009.

[3] H. Zhang, F. L. Lewis, and Z. Qu, "Lyapunov, adaptive, and optimal design techniques for cooperative systems on directed communication graphs," *IEEE Trans. Ind. Electron.*, vol. 59, no. 7, pp. 3026–3041, Jul. 2012.

[4] Y. Su and J. Huang, "Cooperative output regulation of linear multi-agent systems," *IEEE Trans. Autom. Control*, vol. 57, no. 4, pp. 1062–1066, Apr. 2012.

[5] H. Zhang, G. Feng, H. Yan, and Q. Chen, "Observer-based output feedback event-triggered control for consensus of multi-agent systems," *IEEE Trans. Ind. Electron.*, vol. 61, no. 9, pp. 4885–4894, Sep. 2014.

[6] K.-K. Oh, M.-C. Park, and H.-S. Ahn, "A survey of multi-agent formation control," *Automatica*, vol. 53, pp. 424–440, 2015.

[7] Y. Q. Chen and Z. Wang, "Formation control: A review and a new consideration," in *Proc. IEEE/RSJ Int. Conf. Intell. Robot. Syst.*, Edmonton, AB, Canada, 2005, pp. 3181–3186.

[8] W. Ren and R. W. Beard, "Trajectory tracking for unmanned air vehicles with velocity and heading rate constraints," *IEEE Trans. Control Syst. Technol.*, vol. 12, no. 5, pp. 706–716, Sep. 2004.

[9] Z.-P. Jiang and H. Nijmeijer, "Tracking control of mobile robots: A case study in backstepping," *Automatica*, vol. 33, no. 7, pp. 1393–1399, 1997.

[10] J.-M. Yang and J.-H. Kim, "Sliding mode motion control of nonholonomic mobile robots," *IEEE Control Syst. Mag.*, vol. 19, no. 2, pp. 15–23, Apr. 1999.

[11] W. E. Dixon, D. M. Dawson, E. Zergeroglu, and A. Behal, *Nonlinear Control of Wheeled Mobile Robots*. Berlin, Germany: Springer-Verlag, 2001.

[12] A. Gruszka, M. Malisoff, and F. Mazenc, "Bounded tracking controllers and robustness analysis for UAVs," *IEEE Trans. Autom. Control*, vol. 58, no. 1, pp. 180–187, Jan. 2013.

[13] J. P. Desai, J. P. Ostrowski, and V. Kumar, "Modeling and control of formations of nonholonomic mobile robots," *IEEE Trans. Robot. Autom.*, vol. 17, no 6, pp. 905–908, Dec. 2001.

[14] H. G. Tanner, G. J. Pappas, and V. Kumar, "Leader-to-formation stability," *IEEE Trans. Robot. Autom.*, vol. 20, no. 3, pp. 443–455, Jun. 2004.

[15] P. Ögren, M. Egerstedt, and X. Hu, "A control Lyapunov function approach to multi-agent coordination," *IEEE Trans. Robot. Autom.*, vol. 18, no. 5, pp. 847–851, Oct. 2002.

[16] Z. Lin, B. A. Francis, and M. Maggiore, "Necessary and sufficient graphical conditions for formation control of unicycles," *IEEE Trans. Autom. Control*, vol. 50, no. 1, pp. 121–127, Jan. 2005.

[17] K. D. Do, "Formation tracking control of unicycle-type mobile robots with limited sensing ranges," *IEEE Trans. Control Syst. Technol.*, vol. 16, no. 3, pp. 527–538, May 2008.

[18] M. Defoort, T. Floquet, A. Kokosy, and W. Perruquetti, "Sliding-mode formation control for cooperative autonomous mobile robots," *IEEE Trans. Ind. Electron.*, vol. 55, no. 11, pp. 3944–3953, Nov. 2008.

[19] J. Chen, D. Sun, J. Yang, and H. Chen, "A leader-follower formation control of multiple nonholonomic mobile robots incorporating receding-horizon scheme," *Int. J. Robot. Res.*, vol. 29, no. 6, pp. 727–747, 2010.

[20] M. Ou, H. Du, and S. Li, "Finite-time formation control of multiple nonholonomic mobile robots," *Int. J. Robust Nonlinear Control*, vol. 24, no. 1, pp. 140–165, 2014.

[21] P. Wang and B. Ding, "Distributed RHC for tracking and formation of nonholonomic multi-vehicle systems," *IEEE Trans. Autom. Control*, vol. 59, no. 6, pp. 1439–1453, Jun. 2014.

[22] I. Bayezit and B. Fidan, "Distributed cohesive motion control of flight vehicle formations," *IEEE Trans. Ind. Electron.*, vol. 60, no. 12, pp. 5763–5772, Dec. 2013.

[23] N. Léchevin, C. A. Rabbath, and P. Sicard, "Trajectory tracking of leader–follower formations characterized by constant line-of-sight angles," *Automatica*, vol. 42, no. 12, pp. 2131–2141, 2006.

[24] L. Consolini, F. Morbidi, D. Prattichizzo, and M. Tosques, "Leader–follower formation control of nonholonomic mobile robots with input constraints," *Automatica*, vol. 44, no. 5, pp. 1343–1349, 2008.

[25] A. V. Savkin and H. T. Sangani, "Decentralized formation flocking and stabilization for networks of unicycles," in *Proc. 48th IEEE Conf. Decision Control*, Shanghai, China, 2009, pp. 984–989.

[26] A. V. Savkin and H. Teimoori, "Decentralized navigation of groups of wheeled mobile robots with limited communication," *IEEE Trans. Robot.*, vol. 26, no. 6, pp. 1099–1104, Dec. 2010.

[27] T. Liu and Z.-P. Jiang, "Distributed formation control of nonholonomic mobile robots without global position measurements," *Automatica*, vol. 49, no. 2, pp. 592–600, 2013.

[28] T. Liu and Z.-P. Jiang, "Distributed nonlinear control of mobile autonomous multi-agents," *Automatica*, vol. 50, no. 4, pp. 1075–1086, 2014.

[29] E. Panteley and A. Loría, "On global uniform asymptotic stability of nonlinear time-varying systems in cascade," *Syst. Control Lett.*, vol. 33, no. 2, pp. 131–138, 1998.

[30] H. R. Everett, *Sensors for Mobile Robots: Theory and Application*. Natick, MA, USA: A. K. Peters, 1995.

[31] Y. Lin, E. D. Sontag, and Y. Wang, "A smooth converse Lyapunov theorem for robust stability," *SIAM J. Control Optim.*, vol. 34, no. 1, pp. 124–160, 1996.

[32] Y. Kanayama, Y. Kimura, F. Miyazaki, and T. Noguchi, "A stable tracking control method for an autonomous mobile robot," in *Proc. IEEE Int. Conf. Robot. Autom.*, Cincinnati, OH, USA, 1990, pp. 384–389.

[33] W. Ren, "Multi-vehicle consensus with a time-varying reference state," *Syst. Control Lett.*, vol. 56, no. 7, pp. 474–483, 2007.

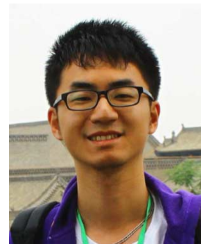

Xiao Yu received the B.S. degree in electrical engineering and automation from Southwest Jiaotong University, Chengdu, China, in 2010, and the M.E. degree in control engineering from Xiamen University, Xiamen, China, in 2013. He is currently working toward the Ph.D. degree in the Department of Mechanical and Biomedical Engineering, City University of Hong Kong, Kowloon, Hong Kong SAR, China.

His research interests include formation control of multiple vehicles and cooperative control of multi-agent systems.

Lu Liu (SM'13) received the Ph.D. degree in the Department of Mechanical and Automation Engineering, The Chinese University of Hong Kong, Shatin, Hong Kong SAR, China, in 2008.

From 2009 to 2012, she was an Assistant Professor with The University of Tokyo, Tokyo, Japan, and then a Lecturer with The University of Nottingham, Nottingham, U.K. She is currently an Assistant Professor with the Department of Mechanical and Biomedical Engineering, City University of Hong Kong, Kowloon, Hong Kong SAR, China. Her research interests include networked dynamical systems, control theory and applications, and biomedical devices.

Dr. Liu was the recipient of the Best Paper Award (Guan Zhaozhi Award) at the 27th Chinese Control Conference in 2008.